Sensor Placement Design for Object Pose Determination with Three Light-Stripe Range Finders

Keiichi Kemmotsu[1] Takeo Kanade

May 10, 1994
CMU-CS-94-152

School of Computer Science
Carnegie Mellon University
Pittsburgh, PA 15213

This research was sponsored by the Avionics Laboratory, Wright Research and Development Center, Aeronautical Systems Division (AFSC), U.S. Air Force, Wright-Patterson AFB, Ohio 45433-6543 under Contract F33615-90-C-1465, ARPA Order No. 7597.

The views and conclusions contained in this document are those of the authors and should not be interpreted as representing the official policies, either expressed or implied, of the U.S. government.

---

[1]This research was performed while the first author was with Carnegie Mellon University. His current address is Advanced Technology Research Center, Mitsubishi Heavy Industries, Ltd., 1-8-1 Sachiura Kanazawa-ku, Yokohama, 236, Japan.

Keywords: object recognition, pose determination, sensor placement, multiple sensors, light-stripe range finder, Monte Carlo method

Abstract

The pose of a polyhedral object can be determined with range data obtained from a set of simple light-stripe range sensors. However, localization results are highly dependent on sensor placement. This paper presents a method for designing an optimal sensor placement of three light-stripe sensors with which to determine the pose of an arbitrarily positioned object. We evaluate a sensor placement on the basis of average performance measures over the whole state space of object pose by a Monte Carlo method. An optimal sensor placement is then selected by another Monte Carlo method which searches for a maximal score function of the performance measures over the whole state of sensor placements.

Contents

1 Introduction **1**

2 Fast Object Recognition with Light-Stripe Range Finders **3**
2.1 Interpretation Tree Search by Geometric Constraints 4
2.2 Computing Transformations 6

3 Geometric Uncertainty in Pose Determination **7**
3.1 Estimating Pose Uncertainty 7
3.2 Example 8

4 Measures for Evaluating Sensor Placements **9**
4.1 Performance Measure in Object Recognition 9
4.2 Performance Measure in Pose Determination 10

5 Sensor Placement Design for Object Pose Determination **11**
5.1 Configuration Space of Sensor Placements 12
5.2 Ranking Sensor Placements 13
5.3 Sensor Placement Design 13
5.4 Simulation Results 14

6 Experimental Results **16**

7 Conclusion **18**

1 Introduction

Recognizing the pose of a three-dimensional (3-D) object in a workspace is a fundamental task in many computer vision applications, including automated assembly, inspection, and bin picking. Many 3-D object recognition systems which use dense range images have been developed [1]. The recognition processes of these systems are very slow, making such techniques impractical for industrial applications. While a dense range image is appropriate for describing a complex scene precisely, scenes in industrial applications can usually be simplified by modifying the environment. This modification enables object recognition using only simple sensors such as light-stripe range finders. Simple range finders are among the fastest and least expensive ways to acquire accurate range data. Multiple range finders viewing an object from different perspectives can usually provide enough constraints to determine the pose of a polyhedral object [17].

The performance of an object recognition system is evaluated with respect to an error rate of object recognition, recognition speed and pose determination error caused by sensing and other errors. One important issue for a system with multiple sensors is that system performance is sensitive to the location of sensors in a workspace, that is, sensor placement. There are two sensing strategies: on-line planning and off-line planning. On-line planning selects the best sensing position sequentially and requires planning and execution time between measurements. On the other hand, off-line planning is desirable for industrial vision tasks because sensing positions are determined all at once before performing the tasks.

In this paper, we present an off-line method for selecting an optimal sensor placement of three simple light-stripe range finders which are used to determine the pose of a polyhedral object. Our method consists of three techniques: object recognition, pose uncertainty estimation and sensor placement evaluation. A method for recognizing an object and estimating the geometric uncertainty of the object's pose was previously described in [16]. In brief, the pose of an object was recognized by matching 3-D line segments obtained by the range finders to model faces based on an interpretation tree search technique with geometric constraints. Then, the geometric uncertainty of the object's pose was estimated by using a relationship between sensing error and pose error.

By combining these methods, we evaluate the goodness of a sensor placement. The state space of the pose of a 3-D object has six degrees of freedom with a uniform probability distribution. Given an object model and a sensor placement of three range finders, an average error rate of object recognition, average recognition time and average position error in pose determination over the state space are estimated by a Monte Carlo method. The given sensor placement can be evaluated by such expected average performance measures.

It is not feasible to explore the entire configuration space which represents an arbitrary sensor placement to find an optimal sensor placement. For simplicity, we assume that the configuration of one range finder in the workspace is defined by three Euler angles which represent the position and orientation of the light plane of the range finder. However,

there are still many degrees of freedom to specify the configuration of three range finders simultaneously. Therefore, another Monte Carlo method is used to select an optimal sensor placement from a configuration space which consists of a finite set of randomly generated sensor placements. Note that the expected average performance of our object recognition and pose determination method under an optimal sensor placement can be characterized completely via the Monte Carlo simulation.

Related Work

The related work on object recognition and pose determination with sparse range data was reviewed in [16]. In brief, Grimson and Lozano-Pérez [9] demonstrated that local unary and binary geometric constraints are very effective in reducing the size of an interpretation tree which represents correspondences between sensed features and model features. A least squares method is usually used to determine the pose of an object [7], [13]. Uncertainty bounds on the object position were obtained geometrically [5], and algebraically [10].

Research on automatic placement of a TV camera and a light source for a vision task has been reported [4],[20],[22],[23]. Assuming that the position of an object is known, acceptable camera positions which simultaneously satisfy the requirements for resolution, field of view, focus and visibility were determined by combining the geometric relationships between the camera positions and those requirements [4], and by using an optimization function [22]. An approach which finds optimal sensor and light source positions in terms of edge visibility was discussed in [23]. A system which automatically generates a layout plan of local windows in the field of view of a camera for visual feedback control tasks by using a singular value decomposition technique was described in [20]. The technique was also used to determine light source positions for a photometric stereo system. However, all the systems described here can be applied only for an object whose pose is known approximately.

Work on planning sensing strategies has been reported [6],[10],[14],[18],[19],[21]. Most of the research, however, has addressed the problem of selecting the next optimal sensing position for object recognition and localization, that is, on-line sequential planning. During initialization, some sensory measurements are necessary to reasonably reduce the number of consistent interpretations of object pose. Then, selection of the next optimal sensing position is achieved by evaluating which sensing position would minimize the ambiguity of the feasible interpretations. The requirements of the initialization were not considered. Compared with on-line sequential planning, off-line batch mode planning for sensing positions is very advantageous. This is because moving a sensor on-line is unacceptable for many industrial applications which require high speed and low cost system configuration. The issue of finding a configuration of multiple sensors to minimize the pose uncertainty of a 2-D object without initial measurements was addressed in [24]. However, a necessary condition for the obtained optimal sensor placement is that it be independent of the object's shape. This is because a sensor placement is defined as the orientations of the sensors relative to

the observed object, and because the sensing error characteristics are sensitive only to the orientations of the sensors. We focus on designing an optimal sensor placement off-line for a given polyhedral object by evaluating sensor placements in terms of object recognition performance and geometric uncertainty in pose determination.

Bayesian decision theory can be used to determine optimal sensing positions for object localization on the basis of average performance, where the average is based on a probability distribution over the state space of a 2-D object [2]. Decision-theoretic principles with geometric models, sensor error models and task models were applied to the problems of optimal sensing strategies and sensor data fusion in [12]. Those approaches handled only the pose uncertainty of a 2-D object with known assignments between sensed features and model features.

Goldberg [8] proposed a stochastic framework for manipulation planning where plans are ranked on the basis of expected cost and demonstrated a stochastically optimal plan for orienting planar parts with a programmable part feeder. He suggested that the stochastic planning can be used to treat the problem of finding an optimal sensor plan for recognizing an object. Stochastic planning is closely related Bayesian decision theory in that both require a probabilistic model to evaluate average performance. However, the difficulty is that we must explicitly describe the effect of a sensing operation with a probability distribution over the state space of a 3-D object. Alternatively, we search for an optimal sensor placement based on the expected average performance of object recognition and pose determination by a Monte Carlo method assuming that the state space of a 3-D object has a uniform probability distribution.

In this section, we introduced the research objective and reviewed related work. Section 2 and 3 summarize our object recognition and pose uncertainty estimation techniques respectively. In Section 4 we define some measures which reflect the system performance of object recognition and pose determination under a sensor placement. Section 5 introduces a method for ranking sensor placements on the basis of expected average performance of object recognition and pose determination, and also design an optimal sensor placement through simulation. In Section 6, we briefly show experimental results with three light-stripe range finders. The complete experiments on pose uncertainty under a designed optimal sensor placement are presented in [16].

2 Fast Object Recognition with Light-Stripe Range Finders

We begin with an object recognition example. A simple light-stripe range finder projects a light plane onto the faces of an object and measures 3-D line segments created by the light-stripe as shown in Figure 1. Three identical range finders are placed in the world

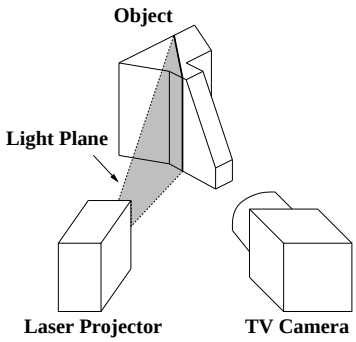

Figure 1: A simple light-stripe range finder.

coordinate frame as shown in Figure 2. The range finders obtain 3-D line segments as shown in Figure 3. Our matching scheme which uses an interpretation tree search assigns the sensed line segments to the corresponding model faces and uses geometric constraints to eliminate inconsistent segment-face pairings. The object's pose is successfully determined as shown in Figure 4. In this section, we briefly describe our object recognition and pose determination technique. Further details are found in [16].

2.1 Interpretation Tree Search by Geometric Constraints

The interpretation tree search technique with local unary and binary geometric constraints finds a consistent set of pairings (S_1, M_{p_1}), (S_2, M_{p_2}), ..., (S_k, M_{p_k}) where M_{p_i} is a model face which corresponds to line segment S_i. The unary constraints check the consistency of a pairing between a line segment and a model face and the binary constraints check the consistency of two pairings.

Our unary and binary constraints for segment-face matching are weaker than those for face-face and edge-edge matching in Grimson's work [11] since line segments carry less information than faces and edges. Therefore, after applying the unary and binary constraints, we apply triplet constraints which check a triplet of pairings between line segments and model faces to prune the interpretation tree more efficiently. We choose three line segments and three model faces under the condition that two of the line segments must intersect each other. Since the two line segments are therefore coplanar, two of the three model faces must be the same. The intersecting line segments can be used to calculate the normal of the model face on which the line segments lie. The normal of the other model face can be obtained by solving a quadratic equation since the normal must be perpendicular to the direction vector of the third line segment. Further details of the triplet constraints may be found in [16].

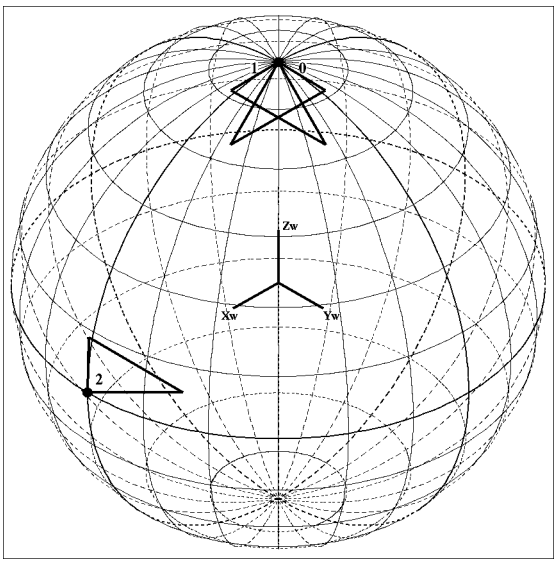

Figure 2: Sensor placement for object recognition. Sensors 0 and 1 are placed on the z axis, directed toward the origin. Their light planes, which are displayed as triangles, are orthogonal. Sensor 2 is placed on the x axis and its light plane lies on the x-y plane.

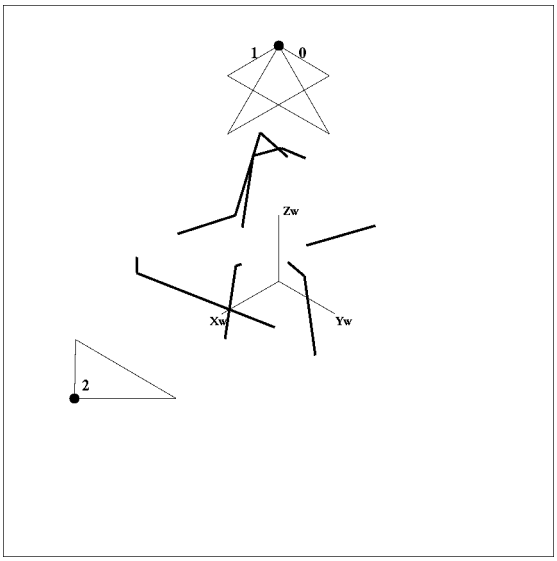

Figure 3: Obtained 3-D line segments on object faces.

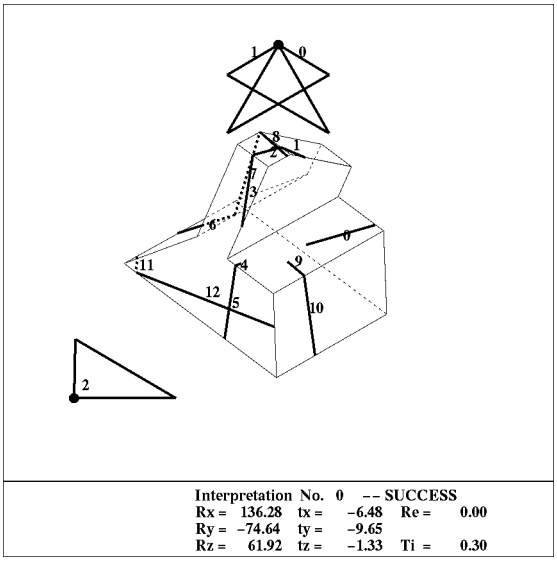

Figure 4: An object recognition result. Estimated transformations $\omega(R_x)$, $\varphi(R_y)$ and $\kappa(R_z)$ are given in degrees and t_x, t_y and t_z are given in millimeters. R_e is the standard deviation of the distances between the endpoints of the line segments and the corresponding object faces. T_i shows the elapsed time in seconds (Sun SPARCstation 2).

2.2 Computing Transformations

Next, we solve for the rotation matrix $\boldsymbol{R}$ and the translation vector $\boldsymbol{t}$ of the transformation which maps points in the model coordinate frame into the world coordinate frame in such a manner that each line segment lies on the corresponding model face. A point $\boldsymbol{p}$ in the world coordinate frame is related to a corresponding point $\boldsymbol{P}$ in the model coordinate frame

$$\boldsymbol{p} = \boldsymbol{R}\boldsymbol{P} + \boldsymbol{t}. \tag{1}$$

Suppose that a line segment S_i, whose endpoints are $\boldsymbol{b}_i$ and $\boldsymbol{e}_i$, corresponds to a model face M_{p_i}. If the point $\boldsymbol{p}$ is on the line segment S_i, the squared distance from the point to the corresponding model face is given by

$$(\Delta d_i)^2 = \left(\boldsymbol{N}_{p_i}^T\left(\boldsymbol{R}^{-1}(\boldsymbol{p}-\boldsymbol{t})\right) + D_{p_i}\right)^2 \tag{2}$$

where $\boldsymbol{N}_{p_i}$ and D_{p_i} are the unit normal and offset of the model face M_{p_i} respectively. The rotation and translation components are therefore obtained by minimizing the sum of the integral of the squared distance along each line segment over all pairings of an obtained feasible interpretation (S_i, M_{p_i}) for $i = 1, \ldots, k$

$$E = \sum_{i=1}^{k} \int_{\boldsymbol{b}_i}^{\boldsymbol{e}_i} (\Delta d_i)^2 ds_i \tag{3}$$

where ds_i is an element of line segment S_i. An initial rotation component for minimization is obtained by using a geometric relationship among three segment-face pairings which include

intersecting line segments. In the event that the three pairings do not include intersecting line segments, a numerical polynomial-based technique [3] is used to obtain a rotation component. Unfortunately, the polynomial-based method is very sensitive to noise and is also computationally expensive since an eighth-degree equation must be solved. On the other hand, the method which uses intersecting line segments is very fast and robust since a rotation component is obtained by solving a quadratic equation in the triplet constraint check. An initial translation component is computed by a least squares method.

3 Geometric Uncertainty in Pose Determination

Now we can determine the pose of an object. However, due to sensing error inherent in measuring line segments, the obtained transformation contains some error which causes uncertainty in the position estimate of the object. This section describes our technique for estimating the pose uncertainty.

3.1 Estimating Pose Uncertainty

Let $\boldsymbol{x}=(t_x,t_y,t_z,\omega,\varphi,\kappa)^T$ be transformation variables, and let $\boldsymbol{s}=(x_1,y_1,z_1,\ldots,x_{2k},y_{2k},z_{2k})^T$ be a vector of endpoint pairs $(x_{2i-1},y_{2i-1},z_{2i-1})$ and (x_{2i},y_{2i},z_{2i}) of line segments S_i for $i=1,\ldots,k$. The pose of an object is determined by minimizing the residual E of equation (3) with respect to $\boldsymbol{x}$. The necessary condition for E to reach an extremum is given as

$$\frac{\partial E}{\partial t_x}=\frac{\partial E}{\partial t_y}=\frac{\partial E}{\partial t_z}=\frac{\partial E}{\partial \omega}=\frac{\partial E}{\partial \varphi}=\frac{\partial E}{\partial \kappa}=0. \tag{4}$$

Now to examine the transformation error $\Delta\boldsymbol{x}$ caused by the sensing error $\Delta\boldsymbol{s}$, we linearize these non-linear equations around the approximate solution $(\boldsymbol{x}_0,\boldsymbol{s}_0)$ which corresponds to the correct transformation and endpoints,

$$\boldsymbol{A}\Delta\boldsymbol{x}\cong-\boldsymbol{B}\Delta\boldsymbol{s} \tag{5}$$

where $\boldsymbol{A}$ is the Hessian matrix of E with respect to $\boldsymbol{x}$ and $\boldsymbol{B}$ is the Jacobian matrix of $\frac{\partial E}{\partial \boldsymbol{x}}$ with respect to $\boldsymbol{s}$.

Furthermore, a relationship between the transformation error $\Delta\boldsymbol{x}$ and the position error $\Delta\boldsymbol{v}_j$ of a vertex $\boldsymbol{v}_j$ is given by

$$\Delta\boldsymbol{v}_j\cong\boldsymbol{D}_j\Delta\boldsymbol{x} \tag{6}$$

where $\boldsymbol{D}_j$ is the Jacobian matrix of $\boldsymbol{v}_j$ with respect to $\boldsymbol{x}$. By substituting equation (5) into equation (6), the covariance matrix $\boldsymbol{C}_{v_j}$ of the vertex $\boldsymbol{v}_j$ is given by

$$\begin{aligned}\boldsymbol{C}_{v_j} &\equiv \boldsymbol{E}(\Delta\boldsymbol{v}_j\Delta\boldsymbol{v}_j^T)\\ &= \boldsymbol{D}_j(\boldsymbol{A}^{-1}\boldsymbol{B})\boldsymbol{C}_s(\boldsymbol{A}^{-1}\boldsymbol{B})^T\boldsymbol{D}_j^T\end{aligned} \tag{7}$$

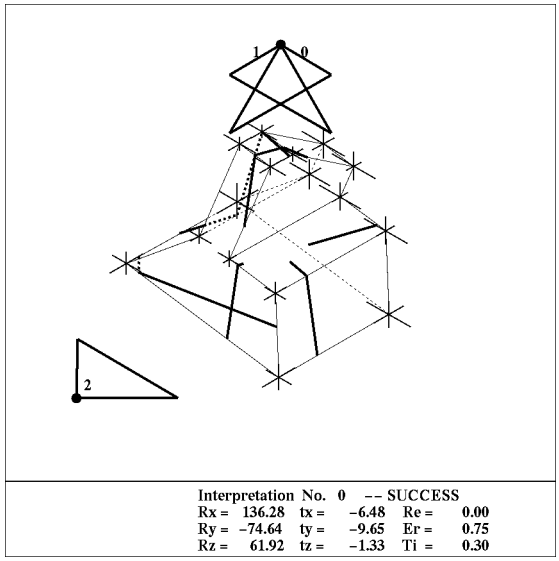

Figure 5: An uncertainty estimation result after recognizing the object. Three bars on each vertex show the uncertainty in pose determination. E_r(mm) is the average position error of all vertices.

where $\boldsymbol{C}_s$ is the covariance matrix of the line segments' endpoint positions. The elements of the covariance matrix $\boldsymbol{C}_{v_j}$ describe the uncertainty in vertex position, and hence the x, y and z components of the position error of each vertex can be approximated as

$$(\Delta v_{j_x}, \Delta v_{j_y}, \Delta v_{j_z}) = (\sqrt{C_{v_j 11}}, \sqrt{C_{v_j 22}}, \sqrt{C_{v_j 33}}). \tag{8}$$

3.2 Example

The following is an example of estimating geometric uncertainty in pose determination. Given the shape of an object, the object's pose in world coordinates, and a sensor placement of three light-stripe range finders, a range finder simulator calculates line segments which would appear on the object. We assume that all endpoints of obtained line segments have the same error (zero mean Gaussian white noise with standard deviation of 1mm). We further assume that any two endpoints are independently measured and that their respective errors are not related (though the mechanism of the sensing error of a range finder is complex in practice [15]). Thus, the covariance matrix $\boldsymbol{C}_s$ of the line segments' endpoint positions becomes the identity matrix. We can estimate the uncertainty of each vertex of the object with equation (7).

Given a model as shown in Figure 1, a sensor placement as in Figure 2, and the same transformation as in Figure 4, the estimated uncertainty on each vertex of the object is shown in Figure 5. In this figure, the lengths of three bars on each vertex along x, y and z

directions are given by equation (8), and show the uncertainty associated with the position of each vertex.[1]

4 Measures for Evaluating Sensor Placements

Given the shape and pose of an object and a sensor placement of three light-stripe range finders, we can decide whether or not the object is recognizable and also we can estimate the uncertainty in the object's pose. In this section, we show that the goodness of a sensor placement can be evaluated through simulation using measures which reflect the performance of object recognition and pose determination assuming the given sensor placement.

4.1 Performance Measure in Object Recognition

We test our object recognition method using simulations. Three hypothetical light-stripe range finders are placed in the world coordinate frame as shown in Figure 2. A polyhedral object as shown in Figure 1 is then placed in the world coordinate frame with a randomly generated transformation $(\boldsymbol{R}_i, \boldsymbol{t}_i)$ for the i th object recognition trial.

As input data for the recognition program, a range finder simulator calculates 3-D line segments which the three light-stripe range finders would get from viewing the object. We obtain feasible interpretations by performing the interpretation tree search with the geometric constraints. If all the estimated vertex positions of each feasible interpretation are near enough to the corresponding correct positions, the interpretation is regarded as correct. The simulation reports that 949 of 1000 trials are successful and that the average recognition time is 0.06 seconds. All failed trials correspond to multiple interpretations which include some correct and some incorrect interpretations.

This simulation suggests that an arbitrary sensor placement can be evaluated with many recognition trials using a Monte Carlo method. The percentage of failed recognition trials and the average computation time per trial indicate how good the sensor placement is for object recognition. One problem is how many trials should be done to evaluate a sensor placement. Simulation results of 1000, 5000 and 10000 trials under five different sensor placements are shown in Table 1. The percentage of failed recognition trials and the recognition time are almost the same regardless of the number of trials. Thus, 1000 trials are sufficient for sensor placement evaluation since the improvements gained by using additional trials are not considered crucial.

[1] For display purpose, those lengths equal $12\Delta v_{j_x}$, $12\Delta v_{j_y}$ and $12\Delta v_{j_z}$ respectively.

Table 1: The percentage of failed trails P_{fail} (%) and the average computation time T (sec) for N =1000, 5000 and 10000 under five different sensor placements.

Sensor Placement	$N = 1000$		$N = 5000$		$N = 10000$	
	P_{fail}	T	P_{fail}	T	P_{fail}	T
No. 1	5.1	0.059	4.9	0.062	4.9	0.061
No. 2	31.1	0.067	31.8	0.071	31.7	0.071
No. 3	4.9	0.087	5.1	0.072	4.8	0.070
No. 4	14.5	0.070	15.2	0.071	15.0	0.069
No. 5	11.1	0.254	10.5	0.225	10.4	0.229

4.2 Performance Measure in Pose Determination

Our method can estimate the position error of an object when the object's pose has been determined. Therefore, a Monte Carlo method is used here again to estimate the average position error of the vertices of an object under a sensor placement with a set of randomly generated transformations.

For the i th transformation, a maximal position error e_i over all vertices of the object is defined as

$$e_i = \max_{1 \le j \le n} \{\sqrt{C'_{v_j 11}}, \sqrt{C'_{v_j 22}}, \sqrt{C'_{v_j 33}}\} \tag{9}$$

where $\boldsymbol{C}'_{v_j}$ is a diagonalized matrix of the covariance matrix $\boldsymbol{C}_{v_j}$ given by equation(7) and n is the number of the vertices. The average position error E for a set of transformations $(\boldsymbol{R}_i, \boldsymbol{t}_i)$ for $i = 1, \ldots, N$ is obtained as

$$E = \frac{1}{N} \sum_{i=1}^{N} e_i. \tag{10}$$

The probable error ΔE of the position error estimate E is defined as

$$\Delta E \equiv \sqrt{\frac{\frac{1}{N}\sum_{i=1}^{N}(e_i)^2 - (E)^2}{N}}. \tag{11}$$

The probable error ΔE is inversely proportional to the square root of the number of trials N, which is regarded as a characteristic of a Monte Carlo method.

Given an object as shown in Figure 1, and a set of transformations, an estimated average position error and its probable error under the five sensor placements from Table 1 are

Table 2: The average position error E (mm) and its probable error ΔE (mm) under five different sensor placements.

Sensor Placement	$N = 1000$		$N = 5000$		$N = 10000$	
	E	ΔE	E	ΔE	E	ΔE
No. 1	1.61	0.024	1.63	0.009	1.63	0.007
No. 2	3.37	0.067	3.47	0.031	3.49	0.023
No. 3	2.04	0.031	2.07	0.015	2.08	0.011
No. 4	2.46	0.051	2.52	0.026	2.51	0.019
No. 5	2.30	0.036	2.30	0.017	2.30	0.012

reported in Table 2. The results show that the average position error varies depending on a sensor placement, and hence the value can be used as a performance measure for evaluating a sensor placement. Judging from the ratio $\Delta E/E$, 1000 trials are sufficient to estimate an average position error.

In summary, a sensor placement can be evaluated with 1000 randomly generated transformations in terms of the following performance measures:

- Percentage of failed recognition trials P_{fail}
- Average recognition time T
- Average position error E.

5 Sensor Placement Design for Object Pose Determination

A sensor placement is assigned a triplet of performance measures (P_{fail}, T, E) using a Monte Carlo method. Our problem is to find a good sensor placement with which an object in an arbitrary pose would be always recognizable with minimal computation time and with minimal pose uncertainty. Therefore, sensor placements must be ranked on the basis of the performance measures to select an optimal sensor placement. In this section, we define a configuration space which represents all possible sensor placements, introduce a scalar function to rank the sensor placements, and then design an optimal sensor placement through simulation.

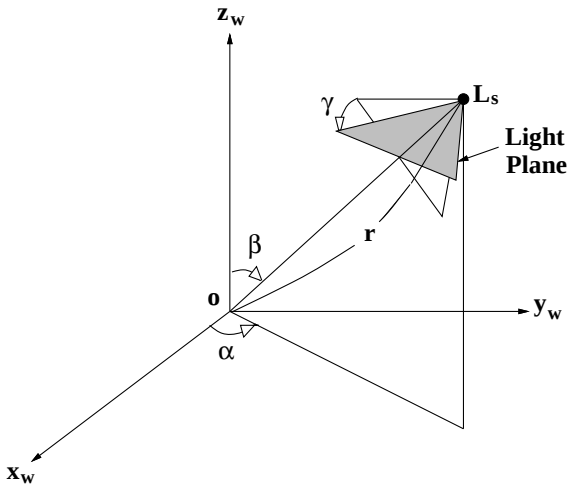

Figure 6: The definition of a light plane. The light plane is defined by three Euler angles (α, β, γ) and a radius r (constant).

5.1 Configuration Space of Sensor Placements

Suppose that we place three light-stripe range finders on the surface of a sphere whose center is located at the origin of the world coordinate frame. The location of each range finder is specified by a light source position, a light plane and a viewpoint which corresponds to a TV camera position. Since there are many degrees of freedom to specify a sensor placement, we assume the following conditions to make computation tractable:

- The range finders can be placed only on the upper hemisphere in practice.
- The radius of the sphere is constant according to the size of a workspace.
- One range finder is placed at the north pole of the sphere, directing to the sphere center and its light plane is aligned with the z-x plane without loss of generality.
- The light planes of the other range finders also pass through the sphere center.
- The light source and viewpoint of each range finder are coincident.[2]

We use three Euler angles α, β and γ to represent a sensor placement θ as shown in Figure 6. The light plane π is given by

$$lx + my + nz = 0 \tag{12}$$

[2] A non-zero baseline complicates simulation by adding occluded line segments to the data. In simulation, however, we can avoid this problem by assuming a zero baseline. Range is computed by intersecting the light plane with the model.

where

$$\begin{aligned} l &= -\cos\alpha\cos\beta\sin\gamma - \sin\alpha\cos\gamma \\ m &= -\sin\alpha\cos\beta\sin\gamma + \cos\alpha\cos\gamma \\ n &= \sin\beta\sin\gamma. \end{aligned} \tag{13}$$

The light source position $\boldsymbol{L}_s$ is $(r\cos\alpha\sin\beta, r\sin\alpha\sin\beta, r\cos\beta)^T$, where r is the radius of the sphere. The ranges of the Euler angles are given by $0 \leq \alpha < 2\pi$, $0 \leq \beta \leq \pi/2$, $0 \leq \gamma < \pi$. Accordingly, a sensor placement θ is described with two sets of Euler angles $(\alpha_1, \beta_1, \gamma_1)$ and $(\alpha_2, \beta_2, \gamma_2)$ corresponding to the two movable sensors. Since a sensor placement is represented by the continuous spaces of such Euler angles, we must partition these spaces into a finite set of sensor placements, which is called the configuration space Θ.

5.2 Ranking Sensor Placements

It is not always possible to find an optimal sensor placement which has the best performance with respect to all the measures simultaneously. Thus, we introduce a scalar function which combines the performance measures to give a score to each sensor placement. Let x_i $(i = 1 \sim 3)$ be values of a triplet of a sensor placement θ_m, and let $\bar{x}_i$ and σ_i be the mean and the standard deviation of x_i over the configuration space. We define a score S_m for the sensor placement θ_m as

$$S_m = \sum_{i=1}^{3} w_i \left(\frac{\bar{x}_i - x_i}{\sigma_i} \right) \tag{14}$$

where w_i is a weight. This equation expresses how far the performance measure x_i of a sensor placement deviates from the mean $\bar{x}_i$. The weight w_i decides how each performance measure contributes to the total score S_m.

Over all sensor placements, the maximal score is

$$S^* = \max_{\Theta} S_m. \tag{15}$$

Hence an optimal sensor placement is defined as a sensor placement with maximal score S^* among the configuration space. By this definition there may be more than one optimal sensor placement due to ties. Thus to be precise we should refer to "an" optimal sensor placement rather than "the" optimal sensor placement according to Goldberg's work [8].

5.3 Sensor Placement Design

We are now ready to design an optimal sensor placement for three light-stripe range finders. However, exploring the entire configuration space of sensor placements is computationally too expensive. Therefore, we introduce another Monte Carlo approach as a strategy of selecting an optimal sensor placement. The procedure is as follows:

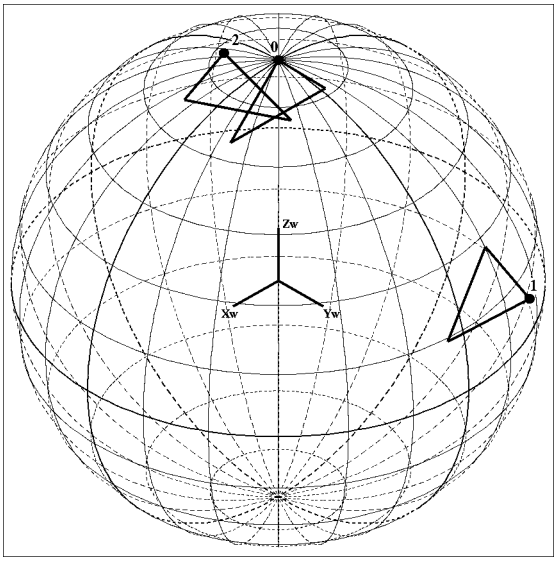

Figure 7: The sensor placement with the highest score for the model No. 1.

- Generate a set of M sensor placements at random with two sets of Euler angles $(\alpha_1, \beta_1, \gamma_1)_m$ and $(\alpha_2, \beta_2, \gamma_2)_m$ for $m = 1, \ldots, M$.
- Estimate the performance measures of each sensor placement.
- Combine them to give a score to the sensor placement.
- Select an optimal sensor placement which has a maximal score among all the sensor placements.

5.4 Simulation Results

We use the object model as shown in Figure 1, and select an optimal sensor placement from 1000 randomly generated sensor placements. The simulation of the m th sensor placement takes as input 1000 different poses of the object model with randomly generated transformations, estimates the performance measures, and computes the score S_m. The sensor placement which has the highest score S^*=13.1 for the object model is shown in Figure 7 (The second highest score is 12.5). The triplet for the sensor placement is (P_{fail}, T, E)=(1.6 %, 0.08 sec, 1.66 mm). Here, the weights w_i are set as (4, 2, 4). The same simulation with a different object model No. 2 as shown in Figure 8 finds the optimal sensor placement as shown in Figure 9.

The triplet values for the optimal sensor placement and the statistics of estimated performance measures for the two models are shown in Table 3. Object recognition for the model No. 1 is more difficult since the mean and median of P_{fail} are much larger than those of the model No. 2. Note that ranking of sensor placements changes according to the weights w_i. The weights w_i must be set by requirements of a vision task.

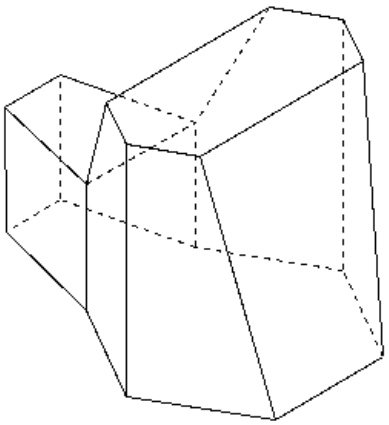

Figure 8: Another object model No.2. The model consists of 12 faces.

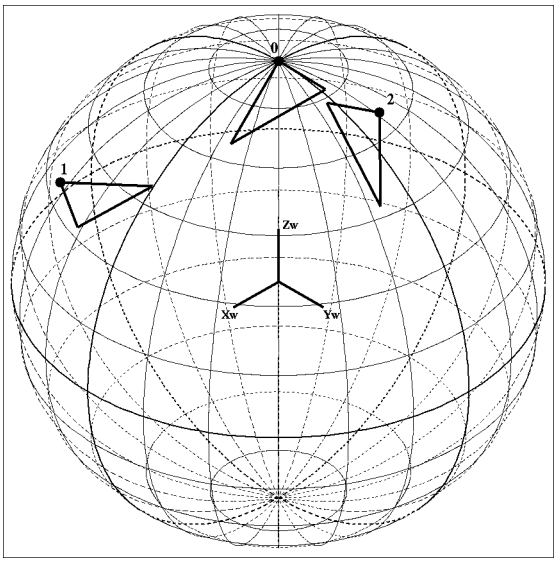

Figure 9: The sensor placement with the highest score for the model No. 2.

Table 3: The triplet values for the optimal sensor placements and the statistics of the performance measures for the two models.

Measures		P_{fail} (%)	T (sec)	E (mm)	S_m
No. 1	Optimal	1.6	0.08	1.66	13.1
	Mean	10.7	0.19	2.28	0.0
	Std	6.0	0.23	0.42	7.9
	Median	9.7	0.09	2.22	1.6
No. 2	Optimal	0.2	0.10	1.67	10.3
	Mean	1.9	0.36	2.33	0.0
	Std	2.7	0.23	0.48	8.3
	Median	1.0	0.30	2.23	2.0

The tendency of ranking of the randomly generated sensor placements is similar for the two models, though the optimal sensor placement is different between them. Relatively good sensor placements for one model are relatively good for the other model. The characteristics of such good sensor placements are summarized as follows:

- Two range finders are closely located, and the associated light planes are almost perpendicular.
- The other range finder is far from the others.

These observations can be supported not only from the point of view of geometric uncertainty in pose determination, but also from a characteristic of our object recognition technique; computation time for recognition with intersecting line segments is absolutely shorter than that without intersecting line segments [17]. Under such a sensor placement, intersecting line segments would more often appear on an object face.

6 Experimental Results

Two simulation results for selecting an optimal sensor placement of three light-stripe range finders were shown in the previous section. This section briefly presents experimental results of recognizing an object and estimating pose uncertainty under the optimal sensor placement. The complete experiments on pose uncertainty under the designed optimal sensor placement are presented in [16].

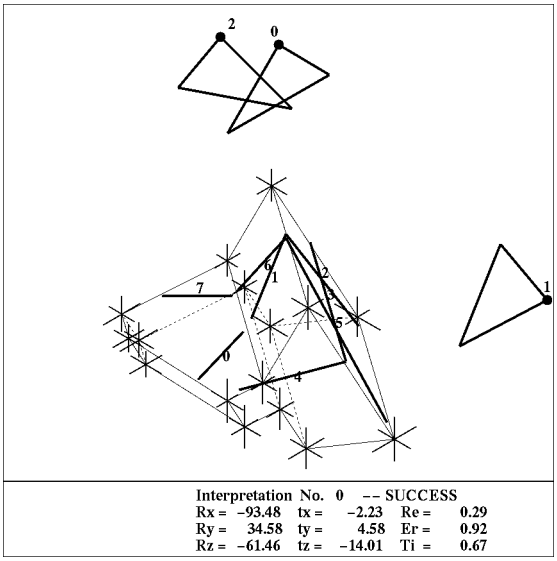

Figure 10: Experimented 3-D line segments and object recognition and position error estimation results for an arbitrary pose.

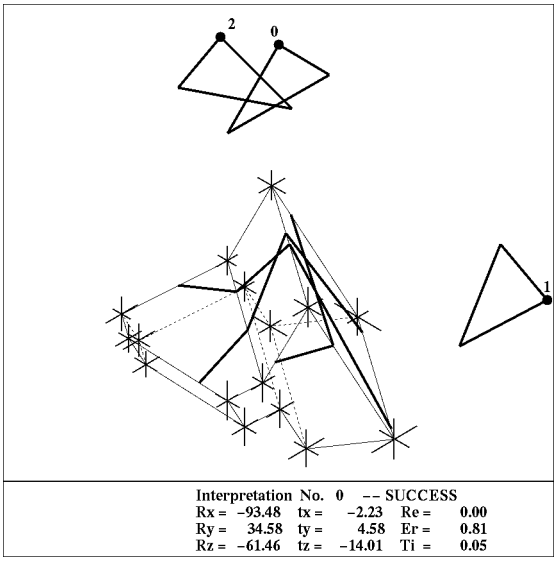

Figure 11: Simulated 3-D line segments and object recognition and position error estimation results for the object's pose shown in Figure 10.

Each light-stripe range finder is composed of a TV camera with a 16 mm lens and a laser diode projector whose wavelength is 670 nm. The laser beam is spread by a cylindrical lens to generate a light plane. The baseline length between the TV camera and the laser projector is about 100 mm. We place three identical range finders above the workspace according to the configuration of the designed optimal sensor placement for the model No. 1 as shown in Figure 7. The distance between each range finder and the workspace center is about 350 mm and each range finder's absolute accuracy for measuring 3-D coordinates is $\pm$ 0.5 mm within the workspace.

An object like the one depicted in Figure 1 is placed at an arbitrary pose in the workspace. Each range finder takes two images (one with the laser diode on, one with the diode off) and obtains 3-D line segments. Figure 10 shows obtained 3-D line segments and object recognition and position error estimation results. For comparison, Figure 11 shows a simulation result with the same object pose under the same sensor placement as the experiment shown in Figure 10. The recognition time in the experiment is 0.67 sec, while only 0.05 sec in the simulation. In the experiment, the geometric constraints used in the interpretation tree search were weakened to allow for error in the measurement, thus, increasing the number of visited nodes. We tried similar experiments with several different poses. A few 3-D line segments were occluded in some experimental results, while the line segments appeared on object faces in corresponding simulation results. This is because the range finder simulator regards the light source and the viewpoint as the same point. Throughout the trials, the experimental results are consistent with the simulation results except for recognition time and occlusion.

7 Conclusion

An object recognition system with simple sensors has two advantages: a simple sensor like a light-stripe range finder is very fast, cheap, reliable and yet provides very accurate data; sensory data are sparse but have enough constraints to determine the pose of a polyhedral object. Finding an appropriate sensor placement is a central problem for such a multi-sensor system. Off-line batch mode planning is indispensable for many industrial vision tasks which require quickness and low cost system configuration.

In this paper, we have presented a method for designing an optimal sensor placement when using three light-stripe range finders to determine the pose of a polyhedral object. We evaluate the goodness of an arbitrary sensor placement with performance measures: an error rate of object recognition, recognition time and pose uncertainty. An optimal sensor placement is selected by ranking randomly generated sensor placements with a Monte Carlo method. Experimental results are in agreement with simulation results. An emphasized point is that the expected average performance of object recognition and pose determination under an optimal sensor placement can be characterized completely via simulation. Our

method is applicable to object pose determination tasks as a designing tool for a sensor placement.

Acknowledgments

The authors would like to thank Carlo Tomasi for useful discussions and comments on this work. Thanks to Jim Moody and Mark DeLouis who made the laser projectors and controller, and to Shin-ichi Yoshimura who helped with the experiments. David Simon read the manuscript carefully and greatly improved its readability. The authors also thank the members of the Vision and Autonomous Systems Center of Carnegie Mellon University for their valuable comments and suggestions.

References

[1] P. J. Besl and R. C. Jain. Three-dimensional object recognition. In *Computing Surveys*, 17(1):75–145, March 1985.

[2] A. Cameron and H. Durrant-Whyte. A Bayesian approach to optimal sensor placement. *The International Journal of Robotics Research*, 9(5):70–88, 1990.

[3] H. H. Chen. Pose determination from line-to-plane correspondences: Existence condition and closed-form solutions. *IEEE Transactions on Pattern Analysis and Machine Intelligence*, 13(6):530–541, June 1991.

[4] C. K. Cowan and P. D. Kovesi. Automatic sensor placement from vision task requirements. *IEEE Transactions on Pattern Analysis and Machine Intelligence*, 10(3):407–416, May 1988.

[5] R. E. Ellis. Geometric uncertainties in polyhedral object recognition. *IEEE Transactions on Robotics and Automation*, 7(3):361–371, June 1991.

[6] R. E. Ellis. Planning tactile recognition paths in two and three dimensions. *The International Journal of Robotics Research*, 11(2):87–111, April 1992.

[7] O. D. Faugeras and M. Hebert. The representation, recognition, and locating of 3-D objects. *The International Journal of Robotics Research*, 5(3):27–52, 1986.

[8] K. Y. Goldberg. *Stochastic Plans for Robotic Manipulation.* PhD thesis, Carnegie Mellon University, August 1990.

[9] W. E. L. Grimson and T. Lozano-Pérez. Model-based recognition and localization from sparse range or tactile data. *The International Journal of Robotics Research*, 3(3):3–35, 1984.

[10] W. E. L. Grimson. Sensing strategies for disambiguating among multiple objects in known poses. *IEEE Journal of Robotics and Automation*, RA-2(4):196–213, December 1986.

[11] W. E. L. Grimson. *Object Recognition by Computer: The Role of Geometric Constraints*. The MIT Press, Cambridge, MA, 1990.

[12] G. Hager and M. Mintz. Computational methods for task-directed sensor data fusion and sensor planning. *The International Journal of Robotics Research*, 10(4):285–313,1991.

[13] B. K. P. Horn, H. M. Hilden, and S. Negahdaripour. Closed-form solution of absolute orientation using orthonormal matrices. *Journal of the Optical Society of America A*, 5(7):1127–1135, July 1988.

[14] S. A. Hutchinson and A. C. Kak. Planning sensing strategies in a robot work cell with multi-sensor capabilities. *IEEE Transactions on Robotics and Automation*, 5(6):765–783, December 1989.

[15] K. Ikeuchi and T. Kanade. Modeling sensors: Toward automatic generation of object recognition program. *Computer Vision, Graphics, and Image Processing*, 48:50–79, 1989.

[16] K. Kemmotsu and T. Kanade. Uncertainty in object pose determination with three light-stripe range measurements. Technical Report CMU-CS-93-100, Carnegie Mellon University, January 1993.

[17] K. Kemmotsu and T. Kanade. Uncertainty in object pose determination with three light-stripe range measurements. In *Proceedings of the IEEE International Conference on Robotics and Automation*, Vol. 3, pages 128–134, May 1993.

[18] S. Lee and H. Hahn. An optimal sensing strategy for recognition and localization of 3-D natural quadric objects. *IEEE Transactions on Pattern Analysis and Machine Intelligence*, 13(10):1018–1037, October 1991.

[19] K. S. Roberts. Robot active touch exploration: Constraints and strategies. In *Proceedings of the IEEE International Conference on Robotics and Automation*, pages 980–985, 1990.

[20] S. Sakane, T. Sato and M. Kakikura. Development of an active vision planning engine towards autonomous hand-eye coordination. In *Proceedings of the 20th International Symposium on Industrial Robots*, pages 103–110, 1989.

[21] J. L. Schneiter and T. B. Sheridan. An automated tactile sensing strategy for planar object recognition and localization. *IEEE Transactions on Pattern Analysis and Machine Intelligence*, 12(8):775–786, August 1990.

[22] K. Tarabanis, R. Y. Tsai and P. K. Allen. Automated sensor planning for robotic vision tasks. In *Proceedings of the IEEE International Conference on Robotics and Automation*, pages 76–82, 1991.

[23] S. Yi, R. M. Haralick, and L. G. Shapiro. Automatic sensor and light source positioning for machine vision. In *Proceedings of the 10th International Conference on Pattern Recognition*, pages 55–59, 1990.

[24] H. Zhang. Optimal sensor placement. In *Proceedings of the IEEE International Conference on Robotics and Automation*, pages 1825–1830, 1992.